Heliyon 10 (2024) e37310

Contents lists available at ScienceDirect

Heliyon

journal homepage: www.cell.com/heliyon

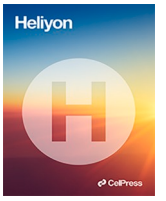

Research article

Spectroscopic, anti-cancer, anti-bacterial and theoretical studies of new bivalent Schiff base complexes derived from 4-bromo-2,6-dichloroaniline

Tarek A. Yousef [a,b,*], Ahmed S. Al-Janabi [c,**]

[a] College of Science, Chemistry Department, Imam Mohammad Ibn Saud Islamic University, Riyadh, 11623, Saudi Arabia
[b] Department of Toxic and Narcotic Drug, Forensic Medicine, Mansoura Laboratory, Medicolegal Organization, Ministry of Justice, Cairo, 11435, Egypt
[c] Department of Chemistry, College of Science, Tikrit University, Tikrit, Iraq

ARTICLE INFO

Keywords:
Schiff base
Oxadiazole
Complexes
DFT
Anti-bacterial

ABSTRACT

In this paper, four new mono-nuclear Ni(II), Pd(II), Pt(II) and Zn(II) complexes were prepared by using a bi-dentate Schiff base ligand, (*E*)-2-(((4-bromo-2,6-dichlorophenyl)imino)methyl)-5-chlorophenol (**BrcOH**), with bivalent ions in a methanol and distil water mixture as solvent in presence of NaOH as base. The structures of the prepared compounds were characterized by spectroscopic techniques (IR and ^{1}H NMR), CHN analysis, and molar conductivity. The M(II) (Ni, Pd and Pt) ions are four-coordinated by a bi-dentate N_2O_2 donor ligand, forming square planar geometry, whereas the Zn(II) is coordinated as a tetrahedral geometry. The newly synthesized compounds, which include the Schiff base ligand and its complexes, underwent antibacterial screening against *E. coli* and *S. aureus*. The results demonstrated a remarkable and noteworthy biological activity of these compounds against these pathogenic bacterial strains. Different binding energies showed good correlation, with Pd showing the strongest binding. Small energy differences indicated high reactivity, with Ni and Pd complexes being the most reactive. Electrophilicity index exhibited electron-accepting properties, with Zn showing the highest reactivity. The dipole moments showed polarity and charge separation, with Pt having the highest polarity. We evaluated the pharmacokinetic properties (ADME) of a ligand and its metal complexes using the Swiss ADME website. The results of the in-silico prediction of physicochemical properties revealed that ten compounds in total adhered to Lipinski's rule.

1. Introduction

Schiff base complexes are coordination compounds that contain a Schiff base ligand coordinated to a metal ion. Schiff bases are organic compounds formed through the condensation reaction between a primary amine and an aldehyde or ketone. This reaction gives rise to the formation of an imine or azomethine functional group (-C=N-), which serves as the foundation of the Schiff base ligand [1–3].

Schiff base complexes have been extensively studied due to their interesting structural, electronic, and magnetic properties. They

* Corresponding author.
** Corresponding author.
E-mail addresses: tayousef@imamu.edu.sa (T.A. Yousef), dr.ahmed.chem@tu.edu.iq (A.S. Al-Janabi).

https://doi.org/10.1016/j.heliyon.2024.e37310
Received 12 May 2024; Received in revised form 10 August 2024; Accepted 30 August 2024
Available online 31 August 2024

find applications in various fields, including catalysis, bioinorganic chemistry, and materials science. The coordination of the Schiff base ligand with a metal ion can influence the reactivity and properties of the resulting complex [3–7]. In Schiff base ligand complexes, the Schiff base ligand coordinates to a metal ion through the nitrogen atom of the imine group with/or without other donor atoms such as oxygen, sulfur, and phosphorus. This coordination can occur in various geometries, such as tetrahedral, square planar, or octahedral, depending on the metal ion and the ligand environment [6–15].

Schiff bases possess unique characteristics that distinguish them as a special class of organic ligands. These include their flexible entanglement, structural divergence, and ease of coordination to metal ions. These properties contribute to their versatility and make them highly valuable in various applications involving coordination chemistry. Schiff base ligands have become very important because they have azomethine (−C=N−) linkages that make them stable, help them chelate, and give them good biological properties [11–14]. A well-thought-out Schiff base ligand scaffold can make metal complexes more effective as medicines by changing the hard/soft properties of the metal ions that hold them together and the balance of lipophilic/hydrophilic molecules in the complexes. Moreover, numerous Schiff base compounds have been recognized for their potent pharmacological properties, encompassing antidepressant, analgesic, antimicrobial, antiviral, and antitumor activities. These compounds have shown promising potential in the field of medicine and hold significant prospects for the development of novel therapeutic agents [13–20]. In addition, the 2,6-dichloroanilines are useful as intermediates in the manufacture of a wide variety of chemical products including, for example, dyes, pharmaceuticals, and agricultural chemicals. According to is very important to change the pharmacological properties of Schiff base ligands derived from 2,6-dichloroaniline derivative by adding a less harmful metal ion. This could make the possible metal complex more therapeutic and targetable. In continuation of our prior research aimed to develop novel Schiff base complexes. The aim of this study included synthesis, characterization, and theoretical investigations of four novel M(II) complexes with the ligand (E)-2-(((4-bromo-2, 6-dichlorophenyl)imino)methyl)-5-chlorophenol (BrcOH). Additionally, the biological activity of both the BrcOH ligand and its complexes is examined, specifically their antibacterial effects against *Escherichia coli* and *Staphylococcus aureus*.

2. Experimental

2.1. General methods and materials

Explained in detail in the supplementary file.

2.2. Synthesis of Schiff base

The Schiff base ligand (*E*)-2-(((4-bromo-2,6-dichlorophenyl)imino)methyl)-5-chlorophenol (**BrcOH**) was prepared by process designate in literature [21] (Scheme 1)

2.3. Synthesis of Bis(2-(((4-bromo-2,6-dichlorophenyl)imino)methyl)-5-chlorophenolate)nickel complex [Ni(BrcO)$_2$] (1)

A hot solution of (*E*)-2-(((4-bromo-2,6-dichlorophenyl)imino)methyl)-5-chlorophenol (0.100g, 0.266 mmol) in ethanol (15 mL) containing some drops of Et_3N was added to an aqueous solution of nickel chloride hexahydrate (0.032g, 0.133 mmol) in (15 mL), with stirring, a green ppt. Was formed. The mixture was refluxed for 3h, then filtered off, washed with distilled water, and dried under vacuum to give greenish –yellow powder (73 % yield, m.p (^{o}C): 290–292.

The Bis(2-(((4-bromo-2,6-dichlorophenyl)imino)methyl)-5-chlorophenolate) palladium, [Pd(BrcO)$_2$](2), Bis(2-(((4-bromo-2,6-dichlorophenyl)imino)methyl)-5-chlorophenolate)platinum, [Pt(BrcO)$_2$] (3) and Bis(2-(((4-bromo-2,6-dichlorophenyl)imino) methyl)-5-chlorophenolate)zinc, [Zn(BrcO)$_2$] (4) were prepared and isolated employing method above.

2.4. Antibacterial studies

The agar well diffusion method originally described by Bauer [22] was used to find the percentage of activity index for all the free Schiff base and their metal complexes. Chloramphenicol was used as a standard drug. The biological activity was tested against two pathogenic bacteria species {*Escherichia coli* (NCTC 29212), and *Staphylococcus aureus* (MTCC 740) }, at 10^{-3} M concentrations of freshly DMSO of the prepared complexes. The microorganisms were supplied from microbiology Lab., Veterinary Medicine, Tikrit University, Iraq. The results are listed in Table 4.

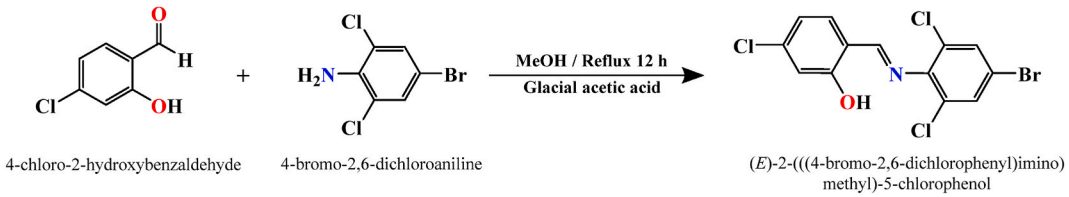

Scheme 1. Preparation of the Schiff base ligand (**BrcOH**).

2.5. DFT studies

Explained in detail in the supplementary file.

3. Results and discussion

The treated of the 4-chloro-2-hydroxybenzaldehyde with the 4-bromo-2,6-dichloroaniline in present glacial acetic acid as catalyst afforded (*E*)-2-(((4-bromo-2,6-dichlorophenyl)imino)methyl)-5-chlorophenol (**BrcOH**) as a solo product in high yield (81 %) (Scheme 1).

Treatment of the Schiff base ligand (**BrcOH**) with metal chlorides correspondingly metal ions to afford complexes of the type [M(BrcO)$_2$] (M^{II}= Ni, Pd, Pt and Zn) in good yield (73–91) % as a solo product (Scheme 2).

The complexes demonstrated complete solubility in DMSO and DMF, while displaying poor solubility in typical organic solvents and insolubility in water. The proposed composition of the M(II) complexes was in good agreement with the analytical results. The findings indicated a stoichiometry of 1:2 for the metal to ligand ratio in the complexes. Molar conductivity measurements of the complexes (1–4) were conducted in a DMSO solution with a concentration of 0.001 M, and elemental analysis was meticulously carried out and presented in Table 1. Interestingly, the practical elemental analysis values closely matched the calculated values, ensuring the consistency of the results. Notably, the metal complexes exhibited low molar conductivity values, as shown in Table 1, indicating their non-electrolytic properties [23]. This comprehensive characterization provides valuable insights into the distinct solubility profiles and conductivity behaviors of the investigated metal complexes.

3.1. Spectroscopic data

3.1.1. IR spectra data

The IR spectrum of the (E)-2-(((4-bromo-2,6-dichlorophenyl)imino) methyl)-5-chlorophenol displayed the stretching vibration of the hydroxyl group at 3452 cm^{-1}.This band was absent in the IR spectra of the [M(BrcO)$_2$] complexes, which suggested the deprotonation of the hydroxyl group and the bonding of metal ions with the hydroxyl oxygen atom [24,25]. Also, the IR spectra of the prepared compounds showed the azomethine group in the Schiff base ligand at 1634 cm^{-1} which shifted to the 1604 - 1596 cm^{-1} region upon its complexation process with metal ions, indicating coordination of metal with the nitrogen atom of the azomethine group [12,15]. The far IR region in the complexes (1–4), exhibited bands at (498–542) cm^{-1} and (434–489) cm^{-1}, that ascribed to ν(M−O) and ν(M−N), correspondingly [26–29]. Other IR bands are listed in Table 2.

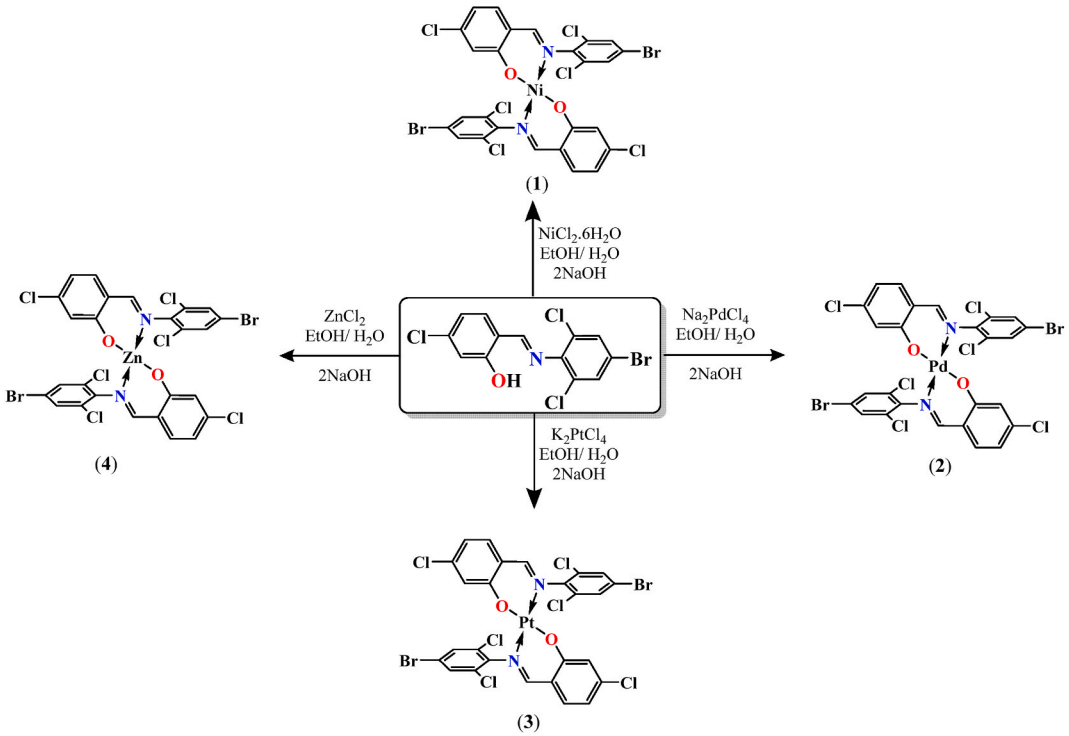

Scheme 2. Preparation of the metal complexes with BrcOH ligand.

Table 1
Physical properties of the free BrcOH ligand and its complexes (**1**–**4**).

Compounds	Color	m.p(°C)	Λ (ohm^{-1}. cm^2. mol^{-1}) in DMSO	Yield %	Elemental analysis calc. (Found)%		
					C	H	N
BrcOH	Off white	139–142	–	81	**41.15** (41.27)	**1.86** (1.93)	**3.69** (3.91)
[Ni(BrcO)$_2$]	Greenish -yellow	290–292	6.1	73	**38.29** (38.21)	**1.48** (1.57)	**3.43** (3.67)
[Pd(BrcO)$_2$]	Pale Brown	276[a]	4.7	77	**36.17** (36.31)	**1.40** (1.62)	**3.24** (3.55)
[Pt(BrcO)$_2$]	Brown	306–304	13.8	83	**32.80** (33.04)	**1.27** (1.50)	**2.94** (3.11)
[Zn(BrcO)$_2$]	White	283[a]	10.7	80	**37.98** (38.14)	**1.47** (1.69)	**3.41** (3.49)

3.1.2. NMR data

The ^{1}H NMR data of the free Schiff base ligand and its complexes are listed in Table 3. The ^{1}H NMR spectrum of the (*E*)-2-(((4-bromo-2,6-dichlorophenyl) imino)methyl)-5-chlorophenol (**BrcOH**) (Fig. 1) exhibited six peaks, four signal as a singlet peak at δ 10.62 (s, 1H), 8.78 (s, 1H), 8.07 (s, 1H), 7.43 (s, 1H) ppm, refer to the proton of hydroxyl group (OH), proton in position (7), proton in position (10,12), and proton in position (2) respectively. In addition, the spectrum showed two doublet peaks at δ 7.79 (d, $J = 8.2$ Hz, 1H), 7.53 (d, $J = 8.2$ Hz, 1H), due to the protons in position (5) and (4), respectively.

The ^{1}H NMR spectra of the [M(BrcO)$_2$] (M^{II}= Ni, Pd, Pt and Zn) complexes in DMSO (Figs. 2 and **3**) clearly showed the deprotonation of the hydroxyl group in the Schiff base ligand and converted to anion ligand. The spectra of the complexes (1–4) showed the protons of the azomethine group at δ (8.41–8.61) ppm region. The spectra additionally revealed distinct peaks corresponding to the protons of the phenyl ring in the aromatic region, with integrations under the signals matching the number of protons. The NMR data, which can be found in Table 3, provides further details regarding these observations.

3.2. Biological activity

The activity of these compounds against two bacterial types (E. *coli* and *S. aureus*) was compared with the obtained results with chlorompinacol as the reference drug. These bactericidal activities are less than those of the standard drug used for comparison purposes. The results achieved from these studies are recorded in Table 4 and Fig. 4. And the activity index (AI) percentage of the biological activity was calculated according to following equation:

$$\text{AI}\ (\%) = \frac{\text{DIZ of tested compound}}{\text{DIZ of standard drug}} * 100$$

The data on the antibacterial activity indicated that the metal complexes are more active than the Schiff base ligand. However, chelation theory does a great job of explaining the increased activity properties after complexation. From the antimicrobial activity results (Table 4) the complexes have shown better activity against pathogenic bacteria than the free ligand. And the activity increased in general according to the following order:

$$\text{Chloramphenicol} > \left[\text{Pt(BrcO)}_2\right] > \left[\text{Zn(BrcO)}_2\right] > \left[\text{Ni(BrcO)}_2\right] > \left[\text{Pd(BrcO)}_2\right] > \text{BrcOH}$$

The antimicrobial activity of complexes [Pt(BrcO)$_2$] is found to be greater but less than that of the standard drug in use. This result is harmonious with those described data for the biological activities in Pd(II) complexes [30–33]. It is suggested that the antibacterial activity of the Pd(II) complex refers to either killing the pathogenic bacteria or inhibiting their growth [30–33].

Chelation theory can be used to explain why prepared compounds have increased reactivity [34]. Chelation, which involves transferring the positive charge of metal ions to groups that donate electrons, can effectively diminish the polarity of these ions. As a consequence of this action, electrons are dispersed throughout the compound's entire structure, improving its affinity for lipids and allowing it to pass through the lipid bilayer of cellular membranes [35]. Also, changing the metal ions with the Schiff base ligand plays a significant role in these complexes' growth inhibitory activity. The activity might be due to the increasing lipophilic nature of these complexes [36–38].

Table 2
Important infrared frequencies (cm^{-1}) of the free BrcOH ligand and its complexes (**1**–**4**).

compounds	ν(C-H) arom./aliph.	ν(C=N)	ν(C=C)	ν(Ph-O)	ν(C-H) bending	ν(M − O)	ν(M − O)
BrcOH	3056w 2987w	1634s	1543s	1106m	754s	–	–
[Ni(BrcO)$_2$]	3032w 2908w	1601s	1567s	1089m	749s	513w	489w
[Pd(BrcO)$_2$]	3030w 2982w	1596s	1544s	1093s	745s	542w	473w
[Pt(BrcO)$_2$]	3058w 2845w	1604s	1533s	1084m	744s	498w	449w
[Zn(BrcO)$_2$]	3080w 2870w	1598s	1520s	1091m	750s	528w	434w

Table 3
Chemical shift in the ^{1}H NMR spectra of the free Schiff base ligand and its complexes.

compounds	Chemical Shift (δ; ppm)
BrcOH	δ 10.62 (s, 1H, OH), 8.78 (s, 1H, H7), 8.07 (s, 2H, H10,12), 7.79 (d, J = 8.2 Hz, 1H, H5), 7.53 (d, J = 8.2 Hz, 1H, H4), 7.43 (s, 1H, H2).
$[Ni(BrcO)_2]$	δ 8.53 (s, 2H, H7), 8.11 (s, 4H, H10,12), 7.76 (d, J = 8.0 Hz, 2H, H5), 7.52 (d, J = 8.0 Hz, 2H, H4), 7.42 (s, 2H, H2).
$[Pd(BrcO)_2]$	δ 8.41 (s, 2H, H7), 8.10 (s, 4H, H10,12), 7.95 (d, J = 8.0 Hz, 2H, H5), 7.53 (d, J = 8.0 Hz, 2H, H4), 7.43 (s, 2H, H2).
$[Pt(BrcO)_2]$	δ 8.61 (s, 2H, H7), 8.04 (s, 4H, H10,12), 7.68 (d, J = 8.0 Hz, 2H, H5), 7.53 (d, J = 8.0 Hz, 1H, H4), 7.40 (s, 2H, H2).
$[Zn(BrcO)_2]$	δ 8.42 (s, 2H, H7), 7.96 (s, 4H, H10,12), 7.78 (d, J = 8.2 Hz, 2H, H5), 7.53 (d, J = 8.2 Hz, 2H, H4), 7.39 (s, 2H, H2).

Table 4
Diameter inhibition zone (DIZ, mm) and activity index (%).

compounds	DIZ (mm)			
	DIZ (E. coli)	AI %(E. coli)	DIZ (S. aureus)	AI %(S. aureus)
BrcOH	10	36	9	29
$[Ni(BrcO)_2]$	18	64	14	45
$[Pd(BrcO)_2]$	15	54	11	35
$[Pt(BrcO)_2]$	21	75	17	55
$[Zn(BrcO)_2]$	20	71	15	48
Chloramphenicol	28	100	31	100

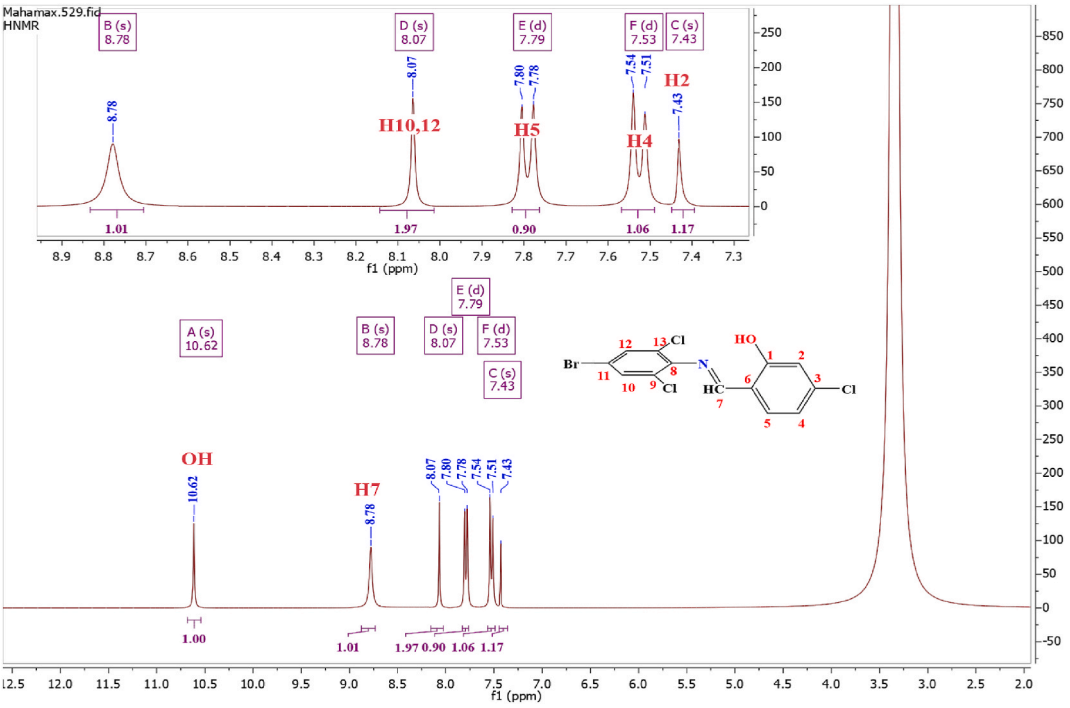

Fig. 1. ^{1}H NMR spectrum of the free BrcOH ligand.

3.3. DFT study

3.3.1. Optimized geometries

The ability to accurately determine equilibrium geometries, identify transition states, and trace reaction pathways is essential for gaining a comprehensive understanding of the underlying molecular mechanisms and energetics involved in chemical processes. Advancements in these areas of geometry optimization are crucial for enhancing the predictive capabilities and reliability of quantum molecular calculations. From the calculated bond lengths of the ligand and its metal complexes (Tables 1S–10S, **Structures 1S-5S** supplementary material) we observed that:

1- There is a large variation in C(7)-N(16), C(6)-O-(9) bond lengths by approximately 0.15–0.2 Å in case of C(7)-N(16) while approximately 0.14–0.18 Å in case of on complexation. It becomes slightly longer as the coordination takes place via N(16) and O(9)

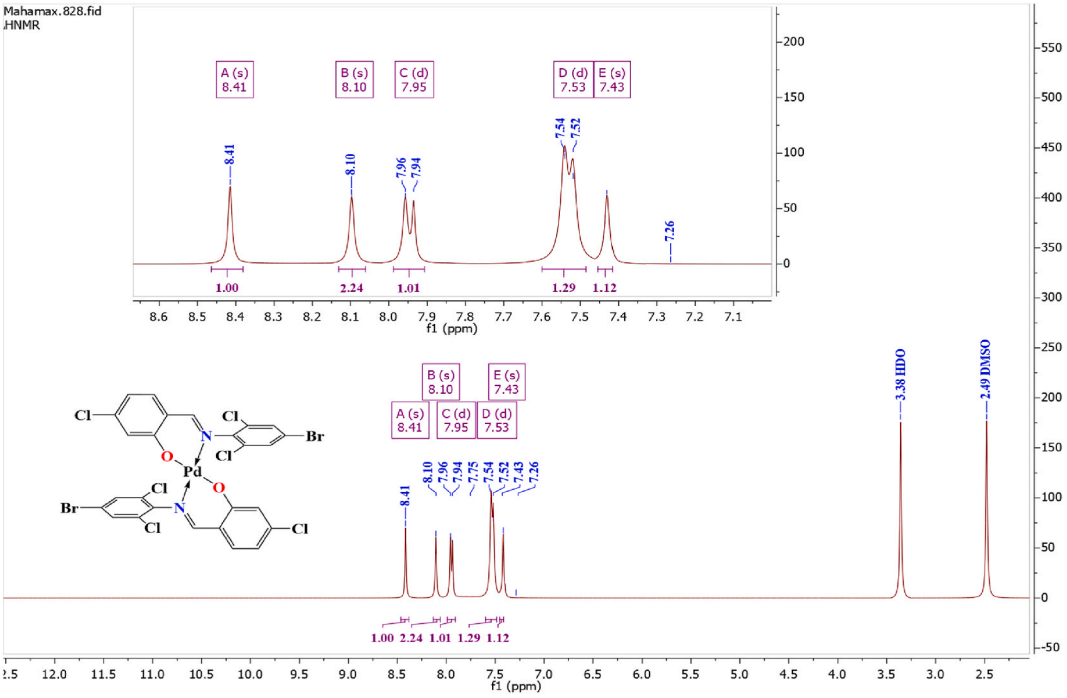

Fig. 2. ^{1}H NMR spectrum of the [Pd(BrcO)$_2$] complex.

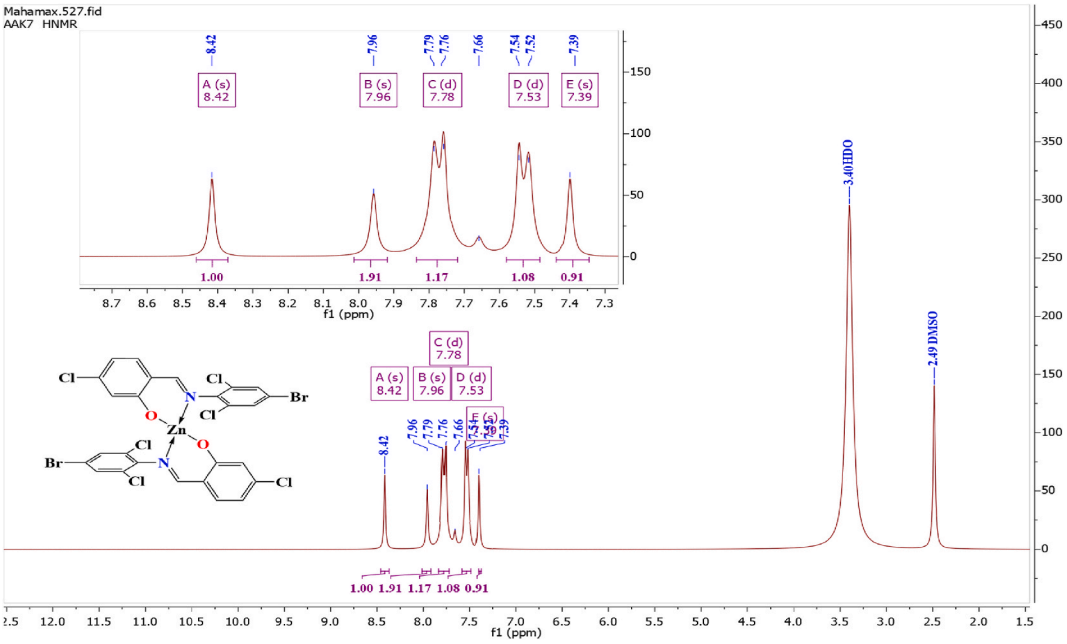

Fig. 3. ^{1}H NMR spectrum of the [Zn(BrcO)$_2$] complex.

atoms [39,40].

2 Coordination with metals significantly affects bond lengths within the ligands.

3 The bond angles of BrcOH are altered somewhat upon coordination but the angles around the metal undergo appreciable variations upon changing the metal centre [40]. The largest change affects C(1)-C(6)-O(9), C(1)-C(7)-N(16), C(7)-N(16)-C(10), and N(16)-C(10)-C(11) angles which are reduced or increased on complex formation as a consequence of bonding.

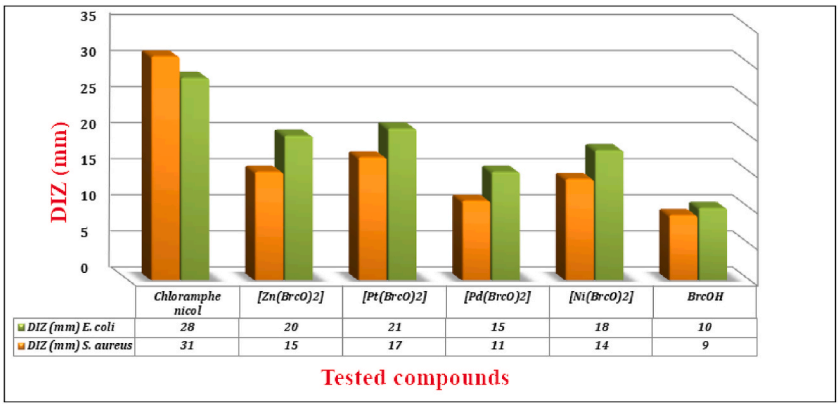

Fig. 4. Biological activity of the free Schiff base ligand and its complexes.

4 The bond angles in all complexes are quite near to a square planar geometry predicting dsp^2 hybridization except $[Zn(BrcO)_2]$ which is quite near to tetrahedral geometry predicting sp^3 hybridization.

3.3.2. Molecular orbitals and quantum chemistry

The frontier molecular orbital provides more details on the optical and electrical features of the materials, moreover, discusses the different kinds of reactions that can occur in conjugated systems [11,41]. In general, the ability to donate an electron is signified by the highest occupied molecular orbital (HOMO), whereas the capacity to gain an electron is represented by LUMO (Figs. 5 and 6). The

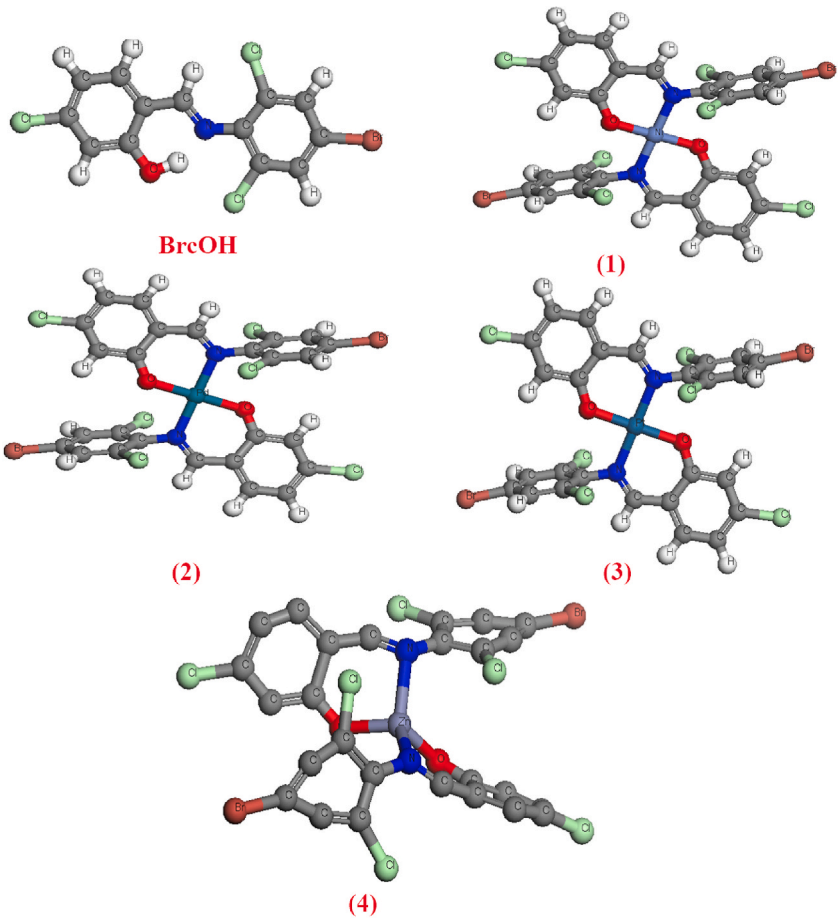

Fig. 5. Optimization structures of the free BrcOH ligand and its complexes (**1**–**4**).

values of HOMO and LUMO energy were used to calculate the several parameters and represented in Table 5.

HOMO energy value and LUMO energy value both have positive correlations with the ionization potential and electron affinity, respectively. EHOMO and ELUMO are related to the free radical scavenging activity of the antioxidant agents. The higher ionization

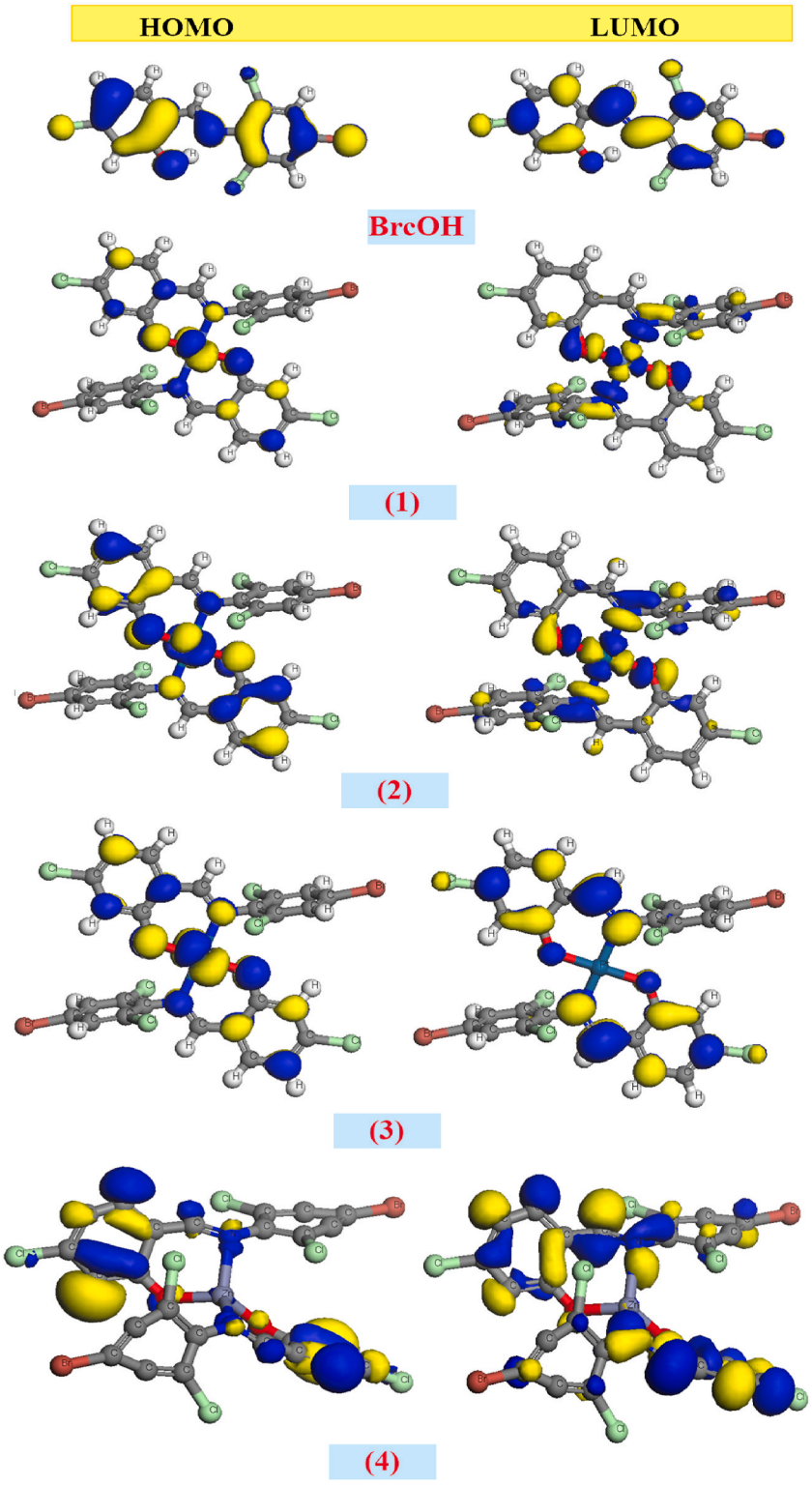

Fig. 6. HOMO and LUMO of the free BrcOH ligand and its complexes (**1**–**4**).

potential and electron affinity of the molecule suggest that it has a higher electronegative value. In most cases, the electron affinity is lower than the ionization potential, indicating that the molecule has a high capacity for electron gain. The global electrophilicity index (ω) measures the molecule's ability to absorb electrons, which is based on the global hardness (η) and chemical potential (μ) values. The high value of the global electrophilicity index (ω) of the molecule indicates good electrophilic behavior [42]. We normally use the differences between the HOMO and LUMO (known as energy gap) to estimate the stability index of the investigated substrate.

The value of the binding energy indicates the stability of the metal-ligand complex. The following table shows that the binding energies of Ni, Pd, Pt, and Zn complexes are negative, indicating positive interactions in binding interactions. Among the four binding metals, Pd has the highest binding energy (−5959.72 kcal/mol), followed by Pt (−5875.15 kcal/mol), Zn (−4620.54 kcal/mol) and Ni (−3493.95 kcal/mol) This follows shows that the Pd complex has the strongest interaction, showing the strongest compared to other complexes. HOMO and LUMO energy levels give an idea of the electron donor and electron acceptor potentials of the complexes. A small energy gap (ΔE) between the HOMO and LUMO numbers indicates a high reactivity. All the complexes have negative HOMO and LUMO energy levels, indicating their ability to accept and donate electrons. Compared to the complexes, Ni has the lowest HOMO energy level (5.52 eV), indicating a strong electron donating ability. On the other hand, the LUMO energy level of Pt is the lowest (−2.72eV), indicating higher electron acceptance than other solids. Smaller gap values indicate higher reactivity and tendency for electron transfer. The smallest differences are for Ni (2.4eV) and Pd (1.26eV), and Pt (1.81eV) and Zn (0.8eV) have the largest activation potentials. The short distance of Ni indicates that electrons are more likely to move and react than other elements.

ΔE is the coefficient (E) of the energy difference between the HOMO and LUMO levels. Shorter lines indicate greater efficiency and greater tendency for electrons to move. The smallest gap covalents are Ni (2.4eV) and Pd (1.26eV), with slightly higher reactions compared to Pt (1.81eV) and Zn (0.8eV). The small difference in Ni indicates that electrons tend to be more mobile and active than other materials. Chemical potential represents the energy required to add or remove electrons from a system. A decrease in chemical potential means a greater tendency to gain or lose electrons in complexes. In this table, Zn has the lowest chemical potential (−4.71eV), indicating that it is more likely to gain or lose electrons than other elements. This suggests that Zn may be more active in electron transfer. Electronegativity refers to the ability of an atom or system to absorb electrons through chemical bonds. The electronegativity values in this table range from 3.61 eV to 4.71 eV. Zn has the highest electronegativity (4.71eV), indicating a stronger absorption than other compounds. In contrast, Ni has the lowest electronegativity (3.61 eV), indicating a relatively weak electron-withdrawing force.

Hardness represents the resistance of the complex to changes in electron density, while softness refers to the tendency of electron density to change the hardest complex in this table (meaning low activity) is Pt (0.89 eV) and Pd (0.91 eV). In contrast, Ni (1.2eV) and Zn (0.4eV) have lower densities, indicating higher activity. The weaknesses followed the same trend, with Ni (0.79eV) and Zn (1.25eV) being weaker (higher product) than Pt (0.55eV) and Pd (0.56eV). These results indicate that the Pt and Pd complexes are relatively stable and less reactive, while the activity of the Ni and Zn complexes is high. Global slowness provides complex reactions when considering multiple molecules. In this table, Zn has the highest global slowness (2.5eV) and shows the largest complex reactivity. Pd has the second highest global slowness (1.59eV), followed by Pt (1.12eV) and Ni (0.83eV). This indicates that Zn has the highest reactive and reactive electron density, while Ni has the lowest. Electrophilicity Index The electrophilic index measures the tendency of complexes to act as electrophiles, accepting electrons in chemical reactions. The electrophilic index values in this table range from 7.32 eV to 27.73 eV. Zn has the highest electromotive index (27.73 eV), indicating a strong tendency to accept electrons and participate in chemical reactions. In contrast, Pt has the lowest electrical resistivity (7.32 eV), indicating low resistance to nucleophilic attack.

The dipole moment indicates the polarity of the complex and the separation of positive and negative charges. From this table, the dipole moment from 0.002 D to 3.070 D is the highest value of the polar moment complex Pt (3.070 d), indicating that the Charge complex has a large charge separation while that of Zn does lowest (0.002 D). Indicating low charge separation. The value of the dipole moment gives an idea of the polarity and possible interactions of the complexes at different sites.

3.3.3. *Mulliken populations*

The Mulliken population analysis results (Fig. 7) presented in the study showed that hydrogen atoms have positive charges, ranging from 0.057 to 0.328 atomic units (a.u.) This positive charge on hydrogen atoms is due to their loss of electrons to surrounding carbon atoms encountered by the. It should be noted that the hydrogen atom had the highest positive charge, which may be related to its

Table 5
Theoretical parameters of the free BrcOH ligand and its complexes (**1**–**4**).

Parameter	BrcOH	1	2	3	4
Binding Energy kcal/mol	−3493.95	−5959.72	−5875.15	−5918.13	−4620.54
E_{HOMO} (eV)	−5.52	−4.32	−4.72	−4.5	−5.11
E_{LUMO} (eV)	−3.12	−3.06	−2.91	−2.72	−4.31
Gap, ΔE	2.4	1.26	1.81	1.78	0.8
Chemical potential (eV)	−4.32	−3.69	−3.82	−3.61	−4.71
Electronegativity	4.32	3.69	3.82	3.61	4.71
Hardness	1.2	0.63	0.91	0.89	0.4
Softness	0.42	0.79	0.55	0.56	1.25
Global Softness	0.83	1.59	1.10	1.12	2.5
Electrophilicity index	7.78	10.81	8.04	7.32	27.73
Dipole moment, (Debye)	2.84	0.002	0.014	0.017	3.07

attachment to the electronegative oxygen atom.

However, nitrogen and oxygen atoms have been reported to have negative Mulliken charges, suggesting that they act as electron acceptors in the molecular system. Some of carbon atoms are negative while most of the carbon atoms were positive. This may be due to their association with electronegative nitrogen and oxygen atoms in the molecular structure [43,44].

3.3.4. Density of states

The density of states (DOS) refers to the number of available electronic states per unit energy interval at a given energy level. It represents the frequency or probability distribution of the electronic states that electrons can occupy within a material. In contrast to estimating the spacing between vibrational frequencies in semiconductors, the DOS simulations enable the computation of the Gaussian probability distribution of the different electronic states as a function of energy, as shown in (Figs. 8 and 9). Understanding the probability of the accessible electronic states per unit volume per unit of energy is crucial for the evaluation of various electronic properties and activities, such as the maximum wavelength of light absorption (λ_{max}), electronic excitation processes, and the total electron scattering behavior in materials with novel designs [43,45].

The DOS calculations were performed theoretically to compare the DOS diagrams of all complexes with the supplementary material (Fig. 1S–3S). We can conclude that.

1 For all complexes, there is an observed increase in the DOS compared to the ligand alone.
2 The increase in DOS suggests higher possible probabilities of electronic transitions in all complexes.
3 The higher DOS of all complexes indicates it is more stable than the ligand alone.

Finally, the complexation of the metals center with the ligand results in an increase in the density of available electronic states. This increased DOS implies a higher probability of electronic transitions occurring within all complexes, which contributes to its enhanced stability compared to the ligand alone.

3.4. ADMET analysis

Indeed, ADMET analysis refers to the comprehensive evaluation of Absorption, Distribution, Metabolism, Excretion, and Toxicity properties of a compound. This analysis provides valuable insights into the pharmacokinetic and toxicological characteristics of a substance, aiding in the assessment of its suitability for use in drug development and other applications. It is a crucial component of drug discovery and development that plays a pivotal role in ensuring that drug candidates are safe, effective, and have the desired pharmacokinetic and pharmacodynamics properties.

Due to their inadequate pharmacokinetic ADMET properties, a significant number of lead-like molecules often encounter failure during clinical trials. In order to mitigate this issue and save both time and costs, in silico examinations are conducted during the drug design and development process, prior to the entry of lead-like molecules into preclinical phases. The pharmacokinetic behavior of the ligand and its metal complexes has been assessed using the SWISS ADME online software. The outputs obtained from this software can be evaluated in accordance with Lipinski's rule of five, which provides valuable guidelines for assessing the drug-likeness of compounds based on their physicochemical properties [41]. Table 6 summarizes the different results of the application of Lipinski's rule. The ligand can penetrate biological membranes, such as the blood-brain barrier, but its metal complex does not. The ligand exhibits high gastrointestinal absorption, indicating efficient transport through the oral route and within the gastrointestinal tract (GIT) and blood-brain barrier (BBB). Additionally, the bioavailability score of 0.55 (>0) suggests that both the ligand and its metal complexes possess significant biological activity. These findings highlight the potential of the ligand and its metal complexes as promising candidates for further exploration in various biomedical applications. In our study, the ligand followed Lipinski's rule with only one violation while in case of metal complexes with 2 violations where at least two violations are considered according to this rule [46].

The pharmacokinetic properties (ADME) of the ligand and its metal complexes were evaluated using the Swiss ADME website (Fig. 10) to determine the pharmacological potential of each of these compounds based on Lipinski's rule. According to the results of the in-silico prediction of physicochemical properties, we observed that ten compounds respect the Lipinski rule. The results obtained in this study are promising, and it is necessary to further studies on these compounds.

4. Conclusion

As part of a systematic study of compounds that have physiological effects, a new Schiff base ligand was made by condensing 4-chloro-2-hydroxybenzaldehyde with 4-bromo-2,6-dichloroaniline. The novel complexes containing Ni(II), Pd(II), Pt(II), and Zn(II) were created from the target ligand (BrcOH). This study used CHN analysis, conductivity measurements, IR, and ^{1}H NMR spectrometry to confirm the structures of the metal and ligand complexes. The newly synthesized Schiff base ligand and metal complexes underwent antimicrobial screening against Staphylococcus aureus and Escherichia coli species. The results were then compared with those of a standard drug to assess their antimicrobial activity. Most complexes exhibited better antimicrobial activities against these organisms than complexes exhibited better antimicrobial activities against these organisms than the original Schiff base ligand. In conclusion, our study examined the stability and reactivity of metal-ligand complexes through various theoretical measurements. Pd showed the strongest binding energy, while Ni exhibited strong electron-donating ability and Pt displayed a higher tendency for electron acceptance. Ni and Pd complexes were found to be highly reactive due to their small energy gaps. Zn demonstrated high electron transfer activity based on chemical potential values. Pt and Pd complexes were relatively stable but less reactive, whereas Ni and Zn

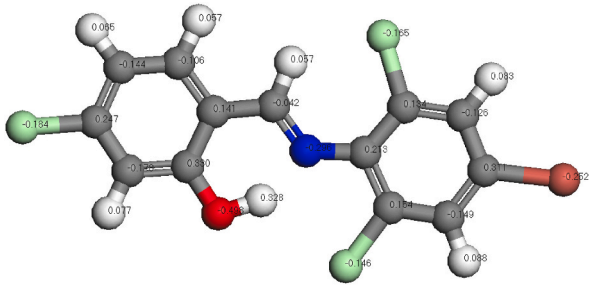

Fig. 7. Mulliken atom charges of BrcOH.

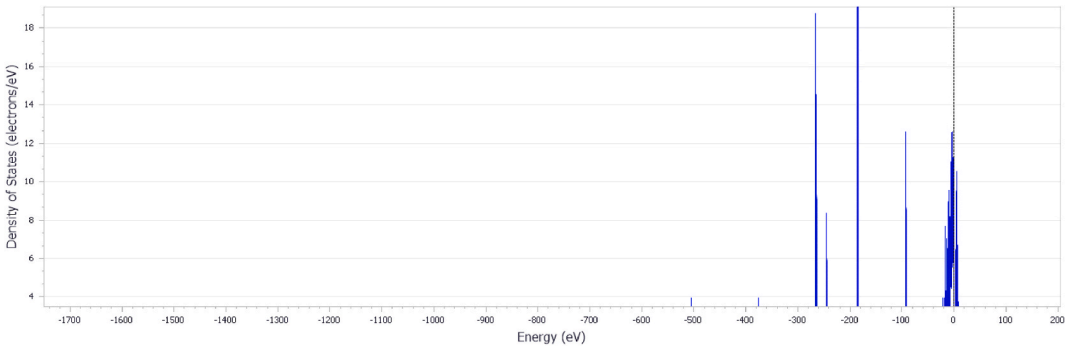

Fig. 8. DOS diagram of BrcOH.

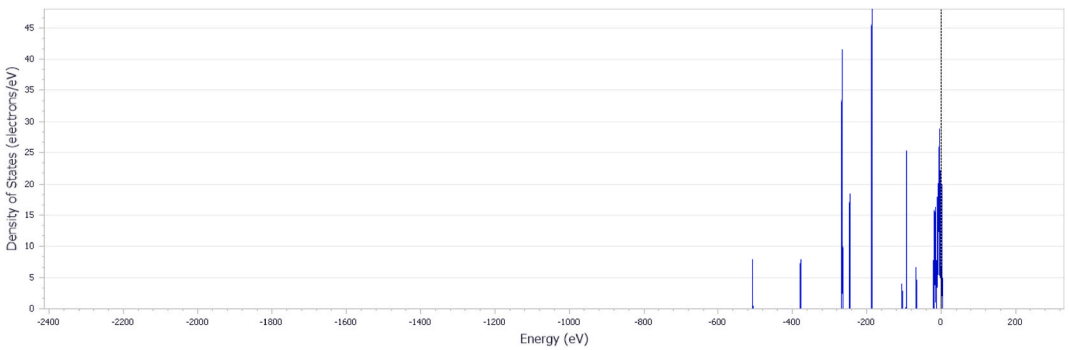

Fig. 9. DOS diagram of $[Ni(BrcO)_2]$ complex.

Table 6
Pharmacological and toxicity prediction of the free BrcOH ligand and its complexes (**1**–**4**).

Parameter		BrcOH	1	2	3	4
Molecular weight		379.46 g/mol	815.61 g/mol	863.33 g/mol	951.99 g/mol	822.29 g/mol
Hydrogen bond donor		1	0	0	0	0
Hydrogen bond acceptor		2	4	4	4	4
Rotatable bonds		2	8	8	8	8
TPSA		32.59 $A^{\circ 2}$	43.18 $A^{\circ 2}$	43.18 $A^{\circ 2}$	43.18 $A^{\circ 2}$	43.18 $A^{\circ 2}$
Lipophilicity		5.04	8.37	8.43	8.54	8.38
Water Solubility		Moderately soluble	Insoluble	Insoluble	Insoluble	Insoluble
Pharmacokinetics	GI absorption	High	Low	Low	Low	Low
	BBB permeant	Yes	No	No	No	No
	Log Kp (skin permeation)	−4.75 cm/s	−3.11 cm/s	−3.40 cm/s	−3.94 cm/s	−3.15 cm/s
Drug likeness (Lipinski)		Yes; 1 violation	No; 2 violations	No; 2 violations	No; 2 violations	No; 2 violations
Bioavailability Score		0.55	0.17	0.17	0.17	0.17

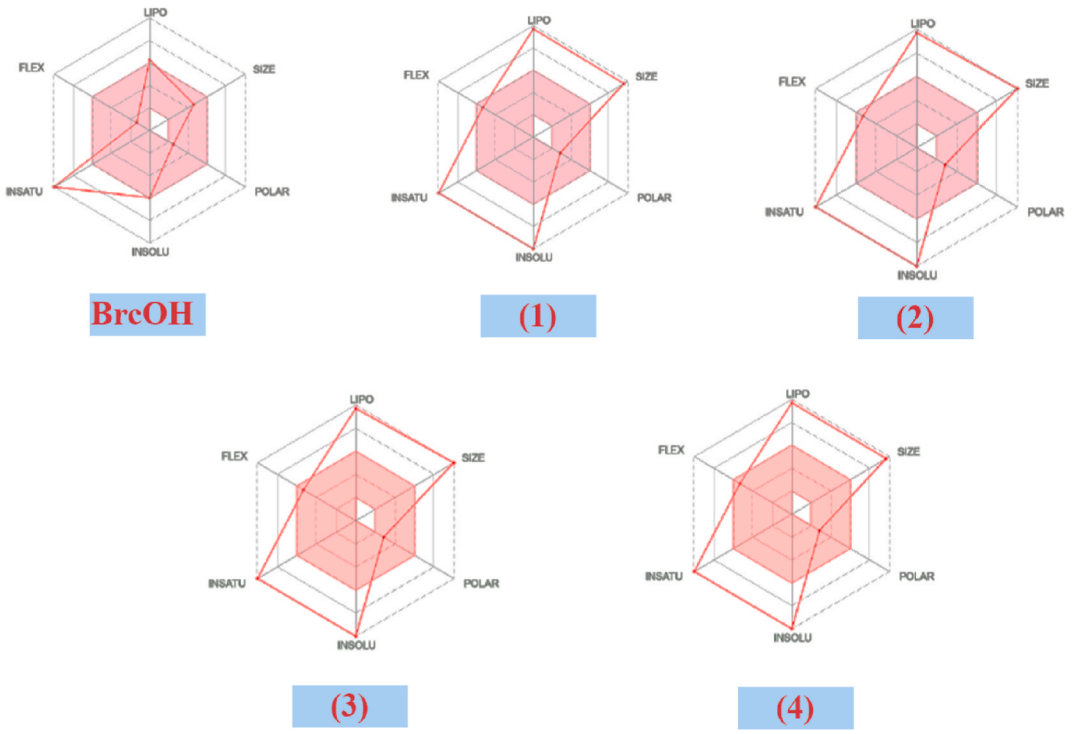

Fig. 10. The Bioavailability Radar enables a first glance at the drug-likeness of ligand and its metal complexes.

complexes displayed higher reactivity according to global hardness and softness measurements. Zn exhibited the highest electrophilicity index, indicating a strong electron-accepting tendency. The dipole moments reflected the polarity and charge separation, with Pt having the highest polarity. These findings contribute to our understanding of the properties and reactivity of metal-ligand complexes, enabling future design and optimization for specific applications. The in-silico prediction of physicochemical properties revealed that ten compounds in total adhered to Lipinski's rule, indicating favorable drug-like characteristics.

CRediT authorship contribution statement

Tarek A. Yousef: Writing – original draft, Validation, Software, Resources, Methodology, Formal analysis, Data curation, Conceptualization. **Ahmed S. Al-Janabi:** Writing – original draft, Resources, Methodology, Investigation, Formal analysis, Data curation, Conceptualization.

Declaration of competing interest

This manuscript has no conflict of interest.

Appendix A. Supplementary data

Supplementary data to this article can be found online at https://doi.org/10.1016/j.heliyon.2024.e37310.

References

[1] E. Sinn, C.M. Harris, Schiff base metal complexes as ligands1, Coord. Chem. Rev. 4 (4) (1969) 391–422. .
[2] K.C. Gupta, A.K. Sutar, Catalytic activities of Schiff base transition metal complexes, Coord. Chem. Rev. 252 (12–14) (2008) 1420–1450. .
[3] A.M. Abu-Dief, I.M. Mohamed, A review on versatile applications of transition metal complexes incorporating Schiff bases, Beni-suef university journal of basic and applied sciences 4 (2) (2015) 119–133. .
[4] M.N. Uddin, S.S. Ahmed, S.R. Alam, Biomedical applications of Schiff base metal complexes, J. Coord. Chem. 73 (23) (2020) 3109–3149. .
[5] W. Zafar, S.H. Sumrra, A.U. Hassan, Z.H. Chohan, A review on 'sulfonamides': their chemistry and pharmacological potentials for designing therapeutic drugs in medical science, J. Coord. Chem. 76 (5–6) (2023) 546–580.
[6] S. Khalid, S.H. Sumrra, Z.H. Chohan, Isatin endowed metal chelates as antibacterial and antifungal agents, Sains Malays. 49 (8) (2020) 1891–1904. .
[7] S.H. Sumrra, M. Anees, A. Asif, M.N. Zafar, K. Mahmood, M.F. Nazar, M.U. Khan, Synthesis, structural, spectral and biological evaluation of metals endowed 1, 2, 4-triazole, Bull. Chem. Soc. Ethiop. 34 (2) (2020) 335–351. .

[8] (a) N. Keshtkar, A. Zamanpour, S. Esmaielzadeh, Bioactive Ni (II), Cu (II) and Zn (II) complexes with an N3 functionalized Schiff base ligand: synthesis, structural elucidation, thermodynamic and DFT calculation studies, Inorg. Chim. Acta. 541 (2022) 121083;
(b) Z.L. You, H.L. Zhu, Syntheses, crystal structures, and antibacterial activities of four Schiff base complexes of copper and zinc, Z. Anorg. Allg. Chem. 630 (15) (2004) 2754–2760.

[9] (a) R. Rajavel, M.S. Vadivu, C. Anitha, Synthesis, physical characterization and biological activity of some Schiff base complexes, J. Chem. 5 (2008) 620–626;
(b) R.S. Joseyphus, M.S. Nair, Antibacterial and antifungal studies on some schiff base complexes of zinc (II), MYCOBIOLOGY 36 (2) (2008) 93–98.

[10] A.S. Al-Janabi, K.H. Oudah, S.A. Aldossari, M.A. Khalaf, A.M. Saleh, M.R. Hatshan, S.F. Adil, Spectroscopic, anti-bacterial, anti-cancer and molecular docking of Pd (II) and Pt (II) complexes with (E)-4-((dimethylamino) methyl)-2-((4, 5-dimethylthiazol-2-yl) diazenyl) phenol ligand, J. Saudi Chem. Soc. 27 (3) (2023) 101619. .

[11] A.S. Al-Janabi, A.F. Al-Bayati, O.A. Altaie, A.O. Elzupir, T.A. Yousef, Co (II), Ni (II), and Zn (II) complexes of 5-methyl-1, 3, 4-oxadiazol-2-amine Schiff base as potential heat shock protein 90 inhibitors: spectroscopic, biological activity, density functional theory, and molecular docking studies, Appl. Organomet. Chem. 36 (12) (2022) e6899. .

[12] W.H. Mahmoud, G.G. Mohamed, O.Y. El-Sayed, Coordination compounds of some transition metal ions with new Schiff base ligand derived from dibenzoyl methane. Structural characterization, thermal behavior, molecular structure, antimicrobial, anticancer activity and molecular docking studies, Appl. Organomet. Chem. 32 (2) (2018) e4051. .

[13] E.A. Bakr, G.B. Al-Hefnawy, M.K. Awad, H.H. Abd-Elatty, M.S. Youssef, New Ni (II), Pd (II) and Pt (II) complexes coordinated to azo pyrazolone ligand with a potent anti-tumor activity: synthesis, characterization, DFT and DNA cleavage studies, Appl. Organomet. Chem. 32 (2) (2018) e4104. .

[14] H.H. Afridi, M. Shoaib, F.A. Al-Joufi, S.W.A. Shah, H. Hussain, A. Ullah, E.U. Mughal, Synthesis and investigation of the analgesic potential of enantiomerically pure schiff bases: a mechanistic approach, Molecules 27 (16) (2022) 5206. .

[15] A.M. Abu-Dief, R.M. El-Khatib, F.S. Aljohani, S.O. Alzahrani, A. Mahran, M.E. Khalifa, N.M. El-Metwaly, Synthesis and intensive characterization for novel Zn (II), Pd (II), Cr (III) and VO (II)-Schiff base complexes; DNA-interaction, DFT, drug-likeness and molecular docking studies, J. Mol. Struct. 1242 (2021) 130693. .

[16] A. Frei, A.P. King, G.J. Lowe, A.K. Cain, F.L. Short, H. Dinh, M.A. Blaskovich, Nontoxic cobalt (III) schiff base complexes with broad-spectrum antifungal activity, Chem.–Eur. J. 27 (6) (2021) 2021–2029. .

[17] R.K. Mohapatra, M.M. El-ajaily, F.S. Alassbaly, A.K. Sarangi, D. Das, A.A. Maihub, T.H. Al-Noor, DFT, anticancer, antioxidant and molecular docking investigations of some ternary Ni (II) complexes with 2-[(E)-[4-(dimethylamino) phenyl] methyleneamino] phenol, Chem. Pap. 75 (2021) 1005–1019. .

[18] M. Sadia, J. Khan, R. Naz, M. Zahoor, S.W.A. Shah, R. Ullah, M. Sohaib, Schiff base ligand L synthesis and its evaluation as anticancer and antidepressant agent, J. King Saud Univ. Sci. 33 (2) (2021) 101331. .

[19] H.A.K. Kyhoiesh, K.J. Al-Adilee, Pt (IV) and Au (III) complexes with tridentate-benzothiazole based ligand: synthesis, characterization, biological applications (antibacterial, antifungal, antioxidant, anticancer and molecular docking) and DFT calculation, Inorg. Chim. Acta. 555 (2023) 121598. .

[20] E.M. Zayed, A.M. Hindy, G.G. Mohamed, Molecular structure, molecular docking, thermal, spectroscopic and biological activity studies of bis-Schiff base ligand and its metal complexes, Appl. Organomet. Chem. 32 (1) (2018) e3952. .

[21] A.S. Al-Janabi, A.O. Elzupir, T.A. Yousef, Synthesis, anti-bacterial evaluation, DFT study and molecular docking as a potential 3-chymotrypsin-like protease (3CLpro) of SARS-CoV-2 inhibitors of a novel Schiff bases, J. Mol. Struct. 1228 (2021) 129454. .

[22] A.W. Bauer, D.M. Perry, W.M. Kirby, Single-disk antibiotic-sensitivity testing of staphylococci: an analysis of technique and results, AMA archives of internal medicine 104 (2) (1959) 208–216. .

[23] W.J. Geary, The use of conductivity measurements in organic solvents for the characterisation of coordination compounds, Coord. Chem. Rev. 7 (1) (1971) 81–122. .

[24] I. Bougossa, D. Aggoun, A. Ourari, R. Berenguer, S. Bouacida, E. Morallon, Synthesis and characterization of a novel non-symmetrical bidentate Schiff base ligand and its Ni (II) complex: electrochemical and antioxidant studies, Chem. Pap. 74 (2020) 3825–3837. .

[25] J.N. Borase, R.G. Mahale, S.S. Rajput, D.S. Shirsath, Design, synthesis and biological evaluation of heterocyclic methyl substituted pyridine Schiff base transition metal complexes, SN Appl. Sci. 3 (2021) 1–13. .

[26] K. Nakamoto, Infrared and Raman Spectra of Inorganic and Coordination Compounds, by John Willey and Sons. Inc, 1986. New York).

[27] S.A. Al-Jibori, A.R. Al-Jibori, H.A. Mohamad, A.S. Al-Janabi, C. Wagner, G. Hogarth, Synthesis and reactivity towards amines of benzisothiazolinate-bridged paddlewheel dimers [M2 (μ-bit) 4· 2H2O](M= Mn, Co, Ni, Cu), Inorg. Chim. Acta. 488 (2019) 152–158. .

[28] A.A. Al-Jibori, S.A. Al-Jibori, A.S. Al-Janabi, Palladium (II) and platinum (II) mixed ligand complexes of metronidazole and saccharinate or benzisothiazolinonate ligands, synthesis and spectroscopic investigation, Tikrit Journal of Pure Science 24 (6) (2019) 26–32. .

[29] A.S. Al-Janabi, R. Zaky, T.A. Yousef, B.S. Nomi, S. Shaaban, Synthesis, characterization, computational simulation, biological and anticancer evaluation of Pd (II), Pt (II), Zn (II), Cd (II), and Hg (II) complexes with 2-amino-4-phenyl-5-selenocyanatothiazol ligand, J. Chin. Chem. Soc. 67 (6) (2020) 1032–1044. .

[30] T.A. Al-Allaf, H. Schmidt, K. Merzweiler, C. Wagner, D. Steinborn, Carboxylation of (DPPF)-MCl2 [DPPF= 1, 1′-bis (diphenylphosphino) ferrocene; M= Pt or Pd] in aqueous and non-aqueous solution: crystal and molecular structures of [Pt (C2O4)(DPPF)] and of [PtCl (NO3)(DPPF)], J. Organomet. Chem. 678 (1–2) (2003) 48–55. .

[31] E. Sajadiyeh, M. Tabatabaee, S.M. Seifati, Z. Derikvand, Cytotoxic effect of palladium (II) complex with 4-amino-5-methyl-2H-1, 2, 4-triazole-3 (4H)-Thione ligand on MCF-7 cell line, Pharmaceut. Chem. J. 54 (2) (2020) 145–147. .

[32] O.D. Al-Mouqdady, A.S. Al-Janabi, M.R. Hatshan, S.A. Al-Jibori, A.S. Fiahan, C. Wagner, Synthesis, characterization, anti-bacterial and anticancer activities of Palladium (II) mixed ligand complexes of 2-mercapto-5-methyl-1, 3, 4-thiadiazole (HmtzS) and phosphines. Crystal structure of [Pd (mtzS) 2 (dppf)]. H2O. EtOH, J. Mol. Struct. 1264 (2022) 133219. .

[33] F. Rivas, A. Medeiros, E.R. Arce, M. Comini, C.M. Ribeiro, F.R. Pavan, D. Gambino, New heterobimetallic ferrocenyl derivatives: evaluation of their potential as prospective agents against trypanosomatid parasites and Mycobacterium tuberculosis, J. Inorg. Biochem. 187 (2018) 73–84. .

[34] B.G. Tweedy, Plant extracts with metal ions as potential antimicrobial agents, Phytopathology 55 (1964) 910–914. .

[35] Y. Anjaneyula, R.P. Rao, Preparation, characterization and antimicrobial activity study on some ternary complexes of Cu(II) with acetyl acetone and various salicylic acids, Synth. React. Inorg. Met. Org. Chem. 16 (1986) 257.

[36] A.S. Al-Janabi, T.A. Yousef, M.E. Al-Doori, R.A. Bedier, B.M. Ahmed, Palladium (II)-salicylanilide complexes as antibacterial agents: synthesis, spectroscopic, structural characterization, DFT calculations, biological and in silico studies, J. Mol. Struct. 1246 (2021) 131035. .

[37] W. Zafar, M. Ashfaq, S.H. Sumrra, A review on the antimicrobial assessment of triazole-azomethine functionalized frameworks incorporating transition metals, J. Mol. Struct. 1288 (2023) 135744. .

[38] M. Amjad, S.H. Sumrra, M.S. Akram, Z.H. Chohan, Metal-based ethanolamine-derived compounds: a note on their synthesis, characterization and bioactivity, J. Enzym. Inhib. Med. Chem. 31 (sup4) (2016) 88–97. .

[39] S. Noreen, S.H. Sumrra, Z.H. Chohan, G. Mustafa, M. Imran, Synthesis, characterization, molecular docking and network pharmacology of bioactive metallic sulfonamide-isatin ligands against promising drug targets, J. Mol. Struct. 1277 (2023) 134780.

[40] T.A. Yousef, G.M. Abu El-Reash, AL-Zahab M. Abu, M.A.A. Safaan, Physicochemical investigations, biological studies of the Cr(III), Mn(II), Fe(III), Co(II), Ni(II), Cu(II), Zn(II), Cd(II), Hg(II) and UO2(VI) complexes of picolinic acid hydrazide derivative: a combined experimental and computational approach, J. Mol. Struct. 1197 (2019) 564–575.

[41] T.A. Yousef, M. Khairy, Synthesis, characterization, optical, DFT, TD DFT studies and in silico ADME predictions of thiosemicarbazone ligand and its Au (III) complex, Orient. J. Chem. 38 (3) (2022). .

[42] Y.B. Choy, M.R. Prausnitz, The rule of five for non-oral routes of drug delivery: ophthalmic, inhalation and transdermal, Pharmaceut. Res. 28 (5) (2011) 943–948.

[43] A.U. Hassan, S.H. Sumrra, W. Zafar, M. Imran, S. Noreen, M. Irfan, Enriching the compositional tailoring of NLO responsive dyes with diversity oriented electron acceptors as visible light harvesters: a DFT/TD-DFT approach, Mol. Phys. 121 (1) (2022).

[44] A.S.M. Al-Janabi, A.O. Elzupir, M.M. Abou-Krisha, T.A. Yousef, New dual inhibitors of SARS-CoV-2 based on metal complexes with schiff-base 4-chloro-3-methyl phenyl hydrazine: synthesis, DFT, antibacterial properties and molecular docking studies, INORGA 11 (2023) 63.
[45] T.A. Yousef, O.K. Alduaij, Sara F. Ahmed, G.M. Abu El-Reash, O.A. El-Gammal, Structural, DFT and biological studies on Cr(III) complexes of semi and thiosemicarbazide ligands derived from diketo hydrazide, J. Mol. Struct. 1125 (2016) 788–799.
[46] C.A. Lipinski, F. Lombardo, B.W. Dominy, P.J. Feeney, Experimental and computational approaches to estimate solubility and permeability in drug discovery and development settings, Adv. Drug Deliv. Rev. 46 (1–3) (2001) 3–26.